11th International Conference on Power Electronics-ECCE Asia
May 22 - 25, 2023 / ICC Jeju, Jeju, Korea

Bi-directional Operation Mode of LLC/CLLC DC/DC Converter for On Board Charger of 800V Battery Systems

Anyeol Jung*, Dongok Moon, Changkyu Bai, Jongho Jang, Minseuk Oh,
Sanghyun Lee, Sunmin Hwang, Hyungtae Moon
HL MANDO, REPUBLIC OF KOREA

***Abstract*-- Global Vehicle OEM's are raising the battery voltage to increase the mileage of electric vehicles and reduce the battery charging time. A bidirectional on-board charger (OBC) is also required for Vehicle to Grid (V2G) and Vehicle to Load (V2L) operation. Recently, ICCU (Integrated Charging Control Unit), a product that integrates OBC and LDC (Low-Voltage DC/DC Converter) circuit and housing, has been developed. In this paper, we propose LLC/CLLC bidirectional DC/DC converter for OBC circuit in 800V battery system. In forward mode, it operates as LLC full-bridge resonant converter to achieve a wide output voltage range. In reverse mode, the DC link voltage can be designed to be lower than in forward mode by operating as a CLLC half-bridge resonant converter. The proposed converter uses SiC-MOSFET, so it satisfies high voltage and is implemented in a small package. The 11 kW prototype of the proposed bidirectional resonant converter was built and tested to verify the proposed operation.**

***Index Terms* — ICCU, On-Board Charger, V2G, V2L.**

I. Introduction

Recently, the research of integrated charger converter units (ICCU) applied to electric vehicles (EVs) has received extensive attention. An overview of the system configuration is shown in Fig.1. Conventionally, on-board charger (OBC) for high-voltage battery and low-voltage DC/DC converter (LDC) for auxiliary battery needs at least two independent converters. ICCU is advantageous in size and cost by implementing two functions in one package, as shown in Fig. 2. In addition, there's a growing demand for bi-directional power flow of on board charger so that the power from battery can be used to support grid or standalone load. [1]-[18]. Dual-active-bridge (DAB) converter and LLC resonant converter have been proposed for bi-directional operation in a wide voltage range of battery. DAB converter can operate in a wide voltage range, but has large switch-off current and low light load efficiency. LLC resonant converter is more efficient than DAB converter due to lower switch-off current in a wide voltage range operation, but cannot operate over a wide voltage range in bi-directional operation due to the asymmetry of the resonant tank.

In order to improve this disadvantage of LLC resonant converter, CLLC resonant converter has been proposed. CLLC resonant converter can operate over a wide voltage range in bi-directional operation due to the symmetry of the resonant tank, and has excellent switching characteristics and thus has good efficiency. Operation of CLLC resonant converter is similar to that of LLC resonant converter, with an LC resonant tank added to the secondary side of the transformer. However, CLLC resonant converter has a more complicated design than LLC resonant converter, and it is difficult to satisfy a desired gain in a desired frequency band in both directions. In this paper, LLC/CLLC mode conversion technique is proposed that operates as LLC resonant converter in the forward mode and compensates for the insufficient voltage gain by operating as CLLC resonant converter with a half-bridge structure in the reverse mode. In order to use the proposed structure, a high-frequency diode and a low-frequency switch are added instead of a high-frequency switch, which can reduce the cost compared to the existing CLLC resonant converter. For half-bridge operation in reverse operation, a secondary-side capacitor is used, and the CLLC resonant converter operates at an almost fixed frequency through DC link variation and has high efficiency. The feasibility of the proposed method was verified with a forward operation 11kW and a reverse operation 5kW prototype.

This paper is organized as follows. Section II shows the system structure of the proposed converter. Bi-directional Converter design procedure is presented in Section III. Section IV shows the experimental results of the 11kW/5kW prototype. Conclusion is then provided in Section V.

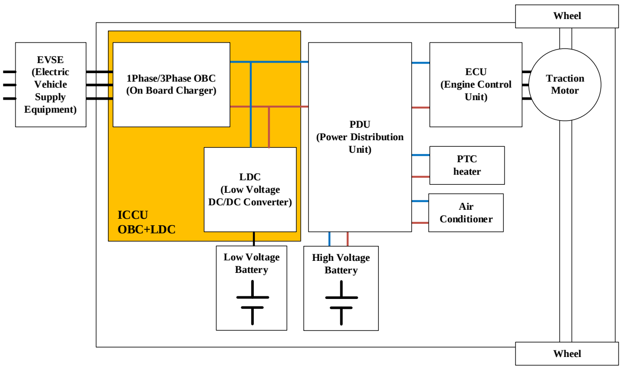

Fig. 1. System Configuration of ICCU.

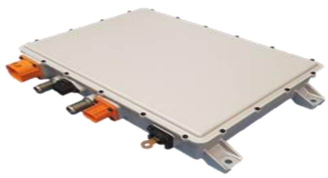

Fig. 2. Package of the ICCU.

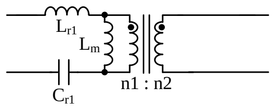

(a) LLC resonant tank

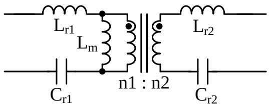

(b) CLLC resonant tank

Fig. 3. Resonant tank of LLC and CLLC converter.

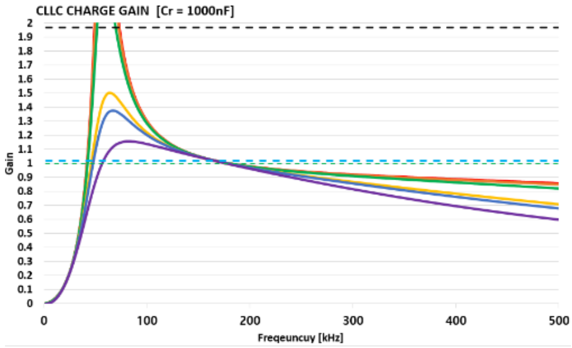

(a) CLLC gain graph with large C_{r2}

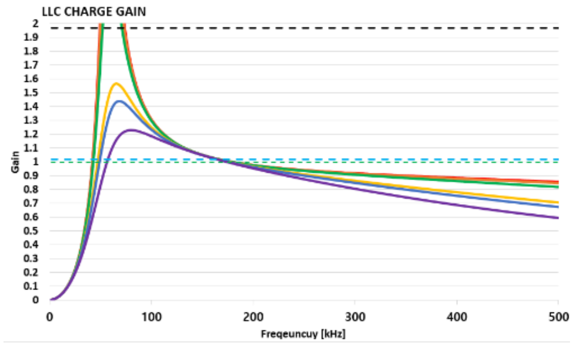

(b) LLC gain graph

Fig. 4. Gain graph of CLLC and LLC Converter according to C_{r2}.

II. System Structure

A. Comparison of LLC and CLLC Resonant Tank Design

Figure 3. shows the LLC and CLLC resonant tanks. As shown in Figure 3(b), the symmetry of the resonant tank is secured by adding the secondary LC of the transformer. The transformer turn ratio, L_{r1}, C_{r1} and L_{r2}, C_{r2} values are used asymmetrically according to the input/output voltage range in the CLLC design. If small L_{r2} and large C_{r2} are used, the CLLC converter can have characteristics similar to LLC. As shown in Figure 4, the larger C_{r2} is, the same as the gain graph of the LLC converter. Using this feature, it is possible to separate the LLC and CLLC designs by operating the CLLC converter in half-bridge mode.

B. Proposed Full Bridge LLC & Half Bridge CLLC Structure

Figure 5. shows the proposed Full bridge LLC and Half Bridge CLLC converters. The proposed converter uses D12 diode instead of high-frequency switch and S12 as low-frequency switch. The proposed converter has the advantage of securing insufficient gain in reverse mode by using a half bridge structure in reverse mode. In forward mode, it operates full-bridge LLC resonant converter. The voltage gain of LLC resonant converter can be controlled as boost mode or buck mode by variable frequency control. In reverse mode, it operate half-bridge CLLC resonant converter. By varying the DC link voltage according to the battery voltage, the CLLC converter operates at a fixed frequency without control.

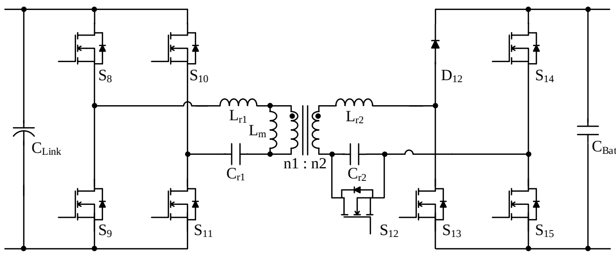

Fig. 5. Proposed LLC Full Bridge and CLLC Half Bridge Converter.

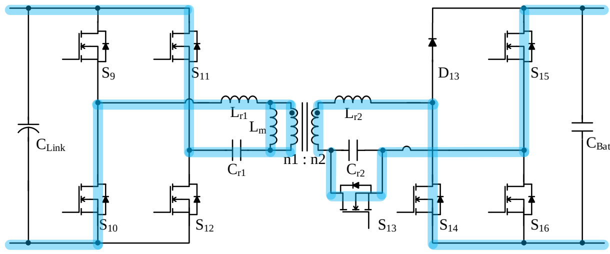
(a) mode I

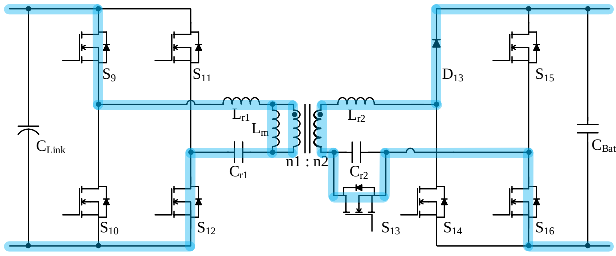
(b) mode II

Fig. 6. Operation mode of the proposed LLC full bridge converter

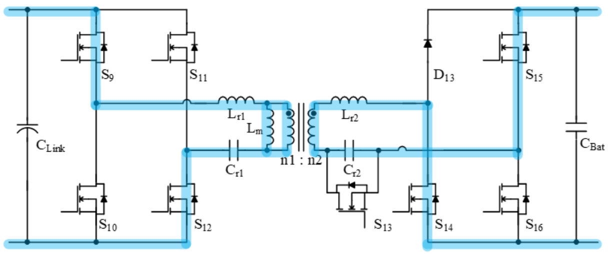
(a) mode I

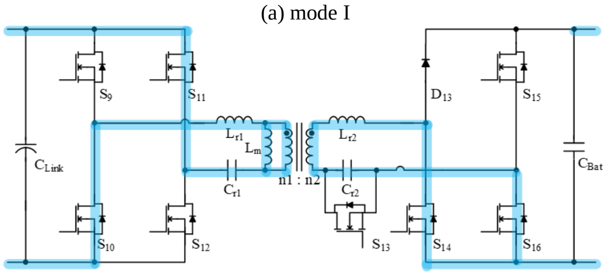
(b) mode II

Fig. 7. Operation mode of the proposed CLLC half bridge converter

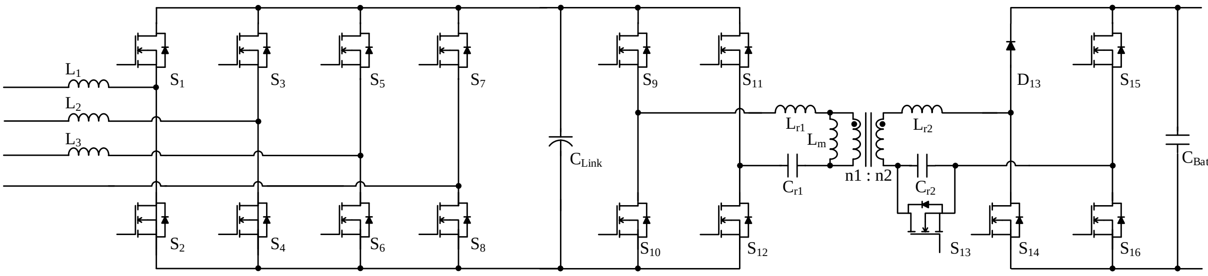

Fig. 8. Proposed bi-directional on-board charger with active front end ac-dc converter.

In order to satisfy the forward and reverse modes, the mode selection switch was added as shown in Fig. 5 and S_{13}. The S_{13} switch can be used to control the conduction path of the secondary resonant capacitor. When charging modes, C_{r2} is not involved in operation by turn-on S_{13}. When reverse modes, C_{r2} is involved in resonance by turn-off S_{13}. Full Bridge LLC performs symmetrical PWM operation. When S_9 and S_{12} are turned on at the same time, S_{10} and S_{11} are turned off. All secondary side SiC MOSFETs are turned off and are conducted in the body-diode pass. S_{13} must be turned on to operate in full bridge rectifier structure. Fig 6. shows the forward mode operation.

Reverse mode operates with CLLC half bridge. First, S_{13} should always be turned off to engage C_{r2} in resonance. In addition, the high side D_{13} of the first leg on the secondary side could be used diode instead of switch. The low side S_{14} should always be turned on. As shown in Figure 7, D_{13} and S_{13} do not affect the discharge operation. This results in a half bridge structure. S_{15} and S_{16} are driven alternately with 50% duty ratio.

C. Proposed On-Board Charger

Fig 8. illustrates the proposed on-board charging system. Active front-end ac-dc converter rectifies the grid voltage and provides power factor correction (PFC), and a following dc-dc stage regulates the intermediate bus voltage into the respective load voltage/current based on the battery state-of-charge (SoC). While the bridgeless totem-pole boost is commonly used for the first stage, proposed LLC-CLLC converter for dc-dc stage. The voltage gain of LLC resonant converter can be controlled as boost mode or buck mode by variable frequency control. In reverse mode, it operate half-bridge CLLC resonant converter. In reverse mode, it operates at fixed frequency without any control.

TABLE I
FORWARD MODE SPECIFICATION

Parameter		Value	Unit
LLC FB Efficiency	η_{LLC_FB}	97	%
DC Link Voltage	V_{dc_min}	630	V
	V_{dc_max}	750	V
Battery Side Power	P_{batt_out}	10500	W
HV Battery Voltage	V_{batt_min}	360	V
	V_{batt_nom}	440	V
	V_{batt_max}	830	V
	I_{batt_max}	25	A
Resonant Frequency	f_r	180	kHz
Minimum Switching Frequency	f_{min}	80	kHz
Coolant Temperature	T_{CT}	65	℃
Ambient	T_A	85	℃

TABLE II
REVERSE MODE SPECIFICATION

Parameter		Value	Unit
CLLC HB Efficiency	η_{CLLC_HB}	95	%
DC Link Voltage	V_{dc_min}	450	V
	V_{dc_max}	750	V
Battery Side Power	P_{batt_out}	5000	W
HV Battery Voltage	V_{batt_min}	550	V
	V_{batt_max}	830	V
	I_{batt_max}	13	A
Switching Frequency	f_{sw}	240	kHz

TABLE III
DESIGN RESULT

Parameter		Value	Unit
Leakage Inductance	L_r	16	μH
Magnetizing Inductance	L_m	144	μH
1st Resonant Capacitor	C_{r1}	49.2	nF
2nd Resonant Capacitor	C_{r2}	196.8	nF
LLC resonant frequency	f_{r1}	180	kHz
LLC peak gain frequency	f_{rp1}	62	kHz
CLLC resonant frequency	f_{r2}	240	kHz
Q factor	Q	0.45	
m value	m	8.5	
Turn ratio	n	1.78	

III. DESIGN BI-DIRECTIONAL CONVERTER

A. Design Specification

The LLC value can be designed based on the conditions of the input / output. In forward mode, the maximum load is 10.5kW and in reverse mode, the maximum load is 5kW. This paper is designed under high rated forward mode. In forward mode, the losses of the devices vary depending on the output voltage conditions. The primary switch and main transformer have the largest losses at the output maximum battery voltage. Conversely, the secondary switch has a high loss due to the high current flowing through the switch at the output minimum battery voltage. Therefore, design and device selection are necessary for the worst condition of each device. Table I and Table II show the specifications for forward mode and reverse mode, respectively.

B. Design Results

In the forward mode, the resonant frequency and peak gain frequency can be calculated as

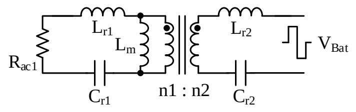

(a) CLLC full bridge resonant tank

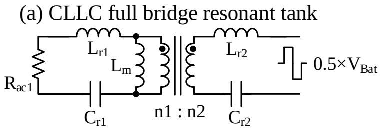

(b) CLLC half bridge resonant tank

Fig. 9. Resonant Tank of CLLC Converter according to operation mode.

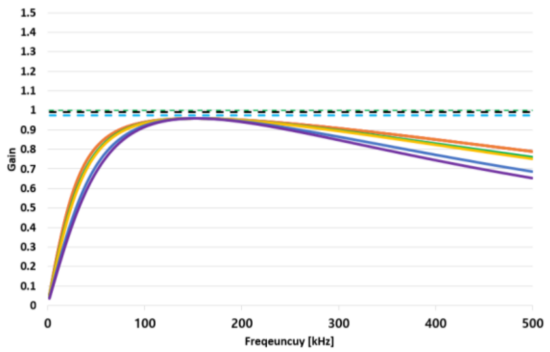

(a) CLLC full bridge resonant tank

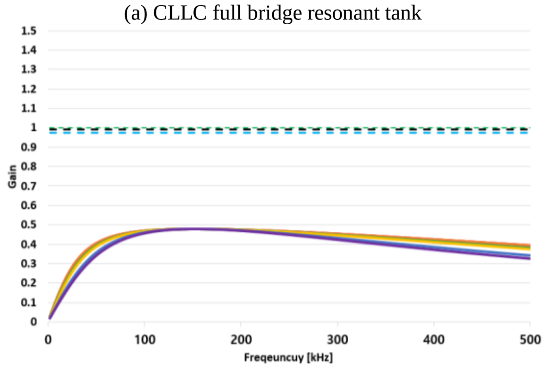

(b) CLLC half bridge resonant tank

Fig. 10. Gain graph of CLLC Converter according to operation mode.

$$f_{r1} = \frac{1}{2\times\pi\sqrt{L_r\times C_{r1}}} \quad (1)$$

$$f_{rp1} = \frac{1}{2\times\pi\sqrt{L_p\times C_{r1}}} \quad (2)$$

Since the half bridge resonant tank transmits half the voltage, the transformer turns ratio is twice as small in reverse mode, as shown in Figure 9. The gain of the resonant tank also decreases proportionally as the transformer turns ratio decreases, as shown in Figure 10. The LLC full bridge voltage gain according to the operating frequency is shown in Fig. 11.

Table III show design results of the proposed resonant converter. LLC optimized design yields a turn ratio of about 1.78. Since a high turn ratio in forward mode creates a high link voltage in reverse mode, the half bridge CLLC structure has the effect of lowering the turn ratio. When using the half bridge structure of the secondary side of the transformer, C_{r2} is absolutely necessary and half bridge is used to operate the reverse mode.

The resonant frequency f_{r2} of the CLLC in the reverse mode can be obtained by selecting the C_{r2} value based on the forward mode design. The operating frequency in this paper is selected as 220kHz for ZVS and secondary ZCS

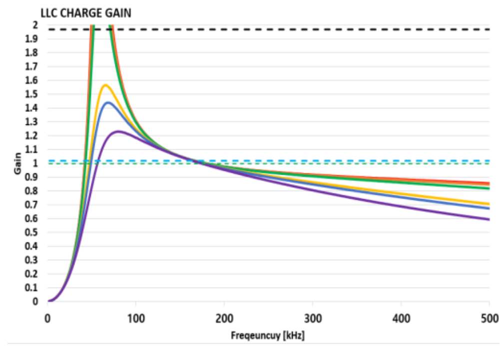

(a) Gain graph of the LLC forward mode

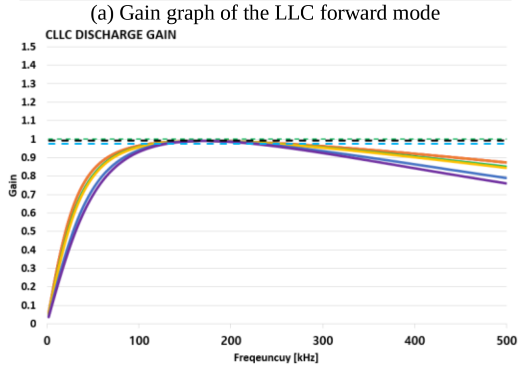

(b) Gain graph of the CLLC reverse mode

Fig. 11. Gain graph of proposed LLC-CLLC Converter according to operation mode.

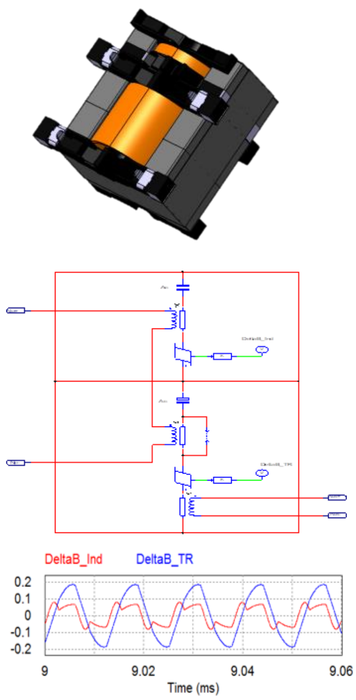

Fig. 12. Magnetics Simulation results at 80kHz using PSIM

operation. In the reverse mode, the resonant frequency can be calculated as

$$f_{r2} = \frac{1}{2\times\pi\sqrt{L_r\times C_{r2}}} \quad (3)$$

The LLC full bridge and CLLC half bridge voltage gain according to the operating frequency is shown in Fig. 11. In reverse mode, the CLLC operates at a fixed frequency at its maximum gain point, where it is most efficient.

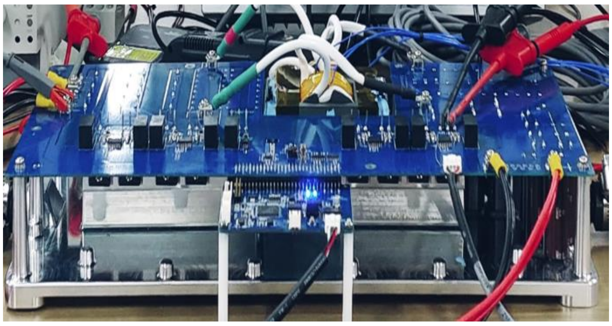

Fig. 13. Prototype of LLC full bridge, CLLC half bridge converter

TABLE IV
TEST CONDITION

Parameter		Value	Unit
Forward mode	Power	10500	W
	V_{link}	750	V
	$V_{bat,min}$	410	V
	$V_{bat,max}$	750	V
Reverse mode	Power	5000	W
	V_{link}	700	V
	V_{bat}	630	V
Coolant Temperature	T_{CT}	25	℃
Ambient	T_A	25	℃

Magnetic transformer concept integrates transformer and leakage inductor. The core type is PQ and the material is PL-17. Core size is customized to deliver 11kW energy. The overall size of the core is 800mm for the X axis, 900mm for the Y axis, and 44mm for the Z axis. The IM Concept is shown in Fig. 12. The magnetic flux density of PL-17 material is 0.41T, which is managed within 0.20T at the minimum operating frequency of 80kHz. The design of the integrated magnetics transformer can be verified by PSIM transformer modeling simulation. The transformer flux density at the maximum output voltage is 0.2T. The IM modeling and simulating results is shown in Fig.12.

IV. EXPERIMENT RESULTS

A prototype 11kW bidirectional LLC-CLLC converter with integrated magnetic transformer was built and tested. The prototype is shown in Fig. 13. Test waveforms are recorded by an LECROY oscilloscope.

Fig. 14 shows the experimental results of the full load test in forward mode. The maximum output voltage is the minimum operating frequency, and the minimum output voltage is the resonance frequency. The test results for each case are shown in Figure 14. Figure 15 (a) shows each waveform at fr and 14 (b) shows each waveform at fsw,min. The turn-off loss of the primary switch can be improved by adjusting the magnetizing inductance. The efficiency was measured by applying the WT1800 Power Analyzer. The efficiency at fr is 95.9% at 11 kW and the efficiency at fsw,min is 96.72%. The reverse mode should be able to operate under light load. Not only the input voltage condition but also the output load condition must be satisfied. Fig. 15 shows the no-load and full-load verification waveforms at 700V input. The reverse mode efficiency under 100W was 80% or less, and the 5kW full load was measured at 97.13%. The reverse mode should be able to operate under light load. Not only the input voltage

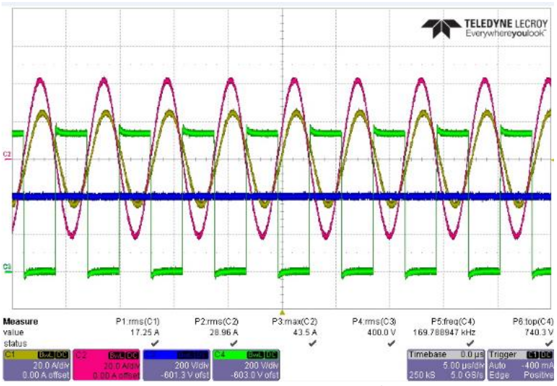

(a) Maximum voltage at f_r

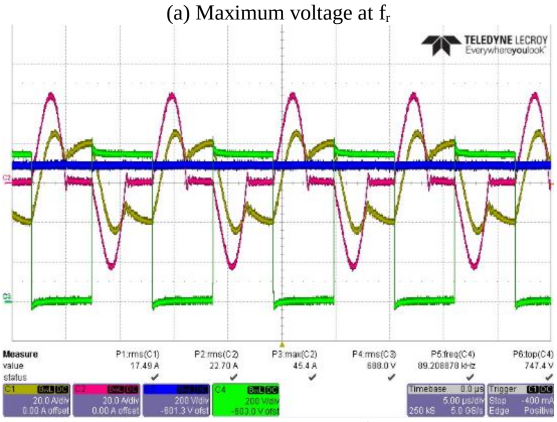

(b) Maximum voltage at $f_{sw,min}$

Fig. 14. Forward mode experimental waveforms.

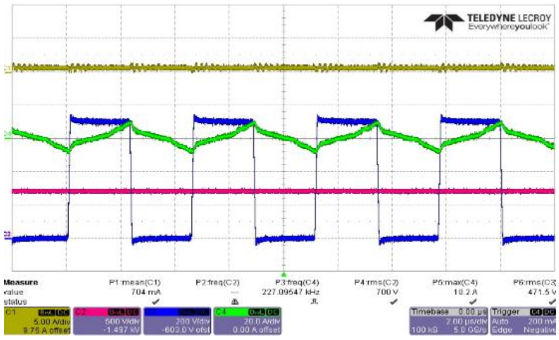

(a) light load at 220kHz

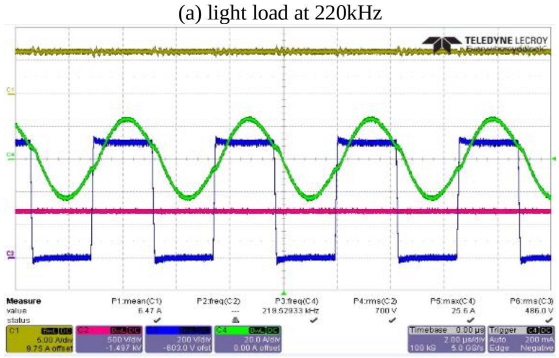

(b) 5kW Full load at 220kHz

Fig. 15. Reverse mode experimental waveforms.

condition but also the output load condition must be satisfied.

V. CONCLUSIONS

This paper has introduced the output voltage range from 360 V to 750 V for battery charger in electrical vehicle applications. In this paper, a mode changing LLC/CLLC bidirectional DC-DC converter with integrated magnetic transformer has been proposed. A 11kW prototype bidirectional DC/DC converter has been implemented to verify its effectiveness. The proposed bi-directional LLC-CLLC converter proved the feasibility by prototype up to 5kW discharge as well as 11kW full load charge. The proposed topology is expected to contribute to cost and size reduction by applying to 800V battery systems of ICCU.

References

[1] Bi-directional on-board charger architecture and control for achieving ultra-high efficiency with wide battery voltage range, Bin Li, Fred C. Lee, Qiang Li and Zhengyang Liu, 2017 IEEE Applied Power Electronics Conference and Exposition, pp 3688 – 3694.

[2] Hao Ma, Yuan Tan, Li Du, Xu Han, Jing Ji, "An Integrated Design of Power Converters for Electric Vehicles" 2017 IEEE 26th International Symposium on Industrial Electronics (ISIE), pp. 600-605.

[3] Murat Yilmaz and Philip T. Krein, "Review of Battery Charger Topologies, Charging Power Levels, and Infrastructure for Plug-In Electric and Hybrid Vehicles," IEEE Trans. Power Electron., vol. 28, no5, pp. 2151–2169, Aug. 2012.

[4] Gang Liu, Dan Li, Jian Qiu Zhang, Bo Hu, Min Li Jia, "Bidirectional CLLC Resonant DC-DC Converter with Integrated Magnetic for OBCM Application", 2015 IEEE International Conference on Industrial Technology (ICIT), pp.946-951.

[5] L. Bing, L. Wenduo, L. Yan et al., "Optimal design methodology for LLC resonant converter," in Applied Power Electronics Conference and Exposition, 2006. APEC '06. Twenty-First Annual IEEE. p. 6 pp.

[6] Biao Zhao ; Qiang Song ; Wenhua Liu ; Yandong Sun "Overview of Dual-Active-Bridge Isolated Bidirectional DC–DC Converter for High- Frequency-Link Power-Conversion System" IEEE Trans. Power Electron., vol. 29, no. 8,pp. 4091–4106, Aug. 2014.

[7] M. H. Kheraluwala and R. W. D. Doncker, "Single phase unity power factor control for dual active bridge converter," in Proc. IEEE Ind. Appl.Soc. Annu. Meet., 1993, pp. 909–916.

[8] M. H. Kheraluwala, R. W. Gascoigne, D. M. Divan, and E. D. Baumann, "Performance characterization of a high-power dual active bridge dc-to dc converter," IEEE Trans. Ind. Appl., vol. 28, no. 6, pp. 1294–1301, Nov./Dec. 1992.

[9] Mi, C. ; Bai, H. ; Wang, C. ; Gargies, S. "Operation, design and control of dual H-bridge-based isolated bidirectional DC-DC converter," Power Electronics, IET (Volume:1 , Issue: 4), pp:507 – 517, Dec. 2008

[10] A. Emadi, "Transportation 2.0," IEEE Power and Energy Magazine, vol. 9, no. 4, pp. 18-29, May 2011.

[11] Texas Instruments, Hybrid and Electric Vehicle Solutions Guide, 2013. [Online]. Available: http://www.ti.com.

[12] B. Bilgin, P. Magne, P. Malysz, Y. Yang, V. Pantelic, M. Preindl, A. Korobkine, W. Jiang, M. Lawford, and A. Emadi, "Making the case for electrified transportation," IEEE Transactions on Transportation Electrification, vol. 1, no. 1, pp. 4-17, June 2015.

[13] A. Emadi, S. S. Williamson, and A. Khaligh, "Power electronics intensive solutions for advanced electric, hybrid electric, and fuel cell vehicular power systems," IEEE Transactions on Power Electronics, vol. 21, no. 3, pp. 567-577, May 2006.

[14] X. Zhang, C. Yao, C. Li, L. Fu, F. Guo, and J. Wang, "A wide bandgap device-based isolated quasi-switched-capacitor DC/DC converter," IEEE Transactions on Power Electronics, vol. 29, no. 5, pp. 2500-2510, May 2014.

[15] I. Aharon and A. Kuperman, "Topological Overview of Powertrains for Battery-Powered Vehicles With Range Extenders," Power Electronics, IEEE Transactions on, vol. 26, pp. 868-876, 2011.

[16] M. Pahlevaninezhad, P. Das, J. Drobnik, P. K. Jain, and A. Bakhshai, "A Novel ZVZCS Full-Bridge DC/DC Converter Used for Electric Vehicles," Power Electronics, IEEE Transactions on, vol. 27, pp. 2752- 2769, 2012.

[17] M. Yilmaz and P. T. Krein, "Review of Battery Charger Topologies, Charging Power Levels, and Infrastructure for Plug-In Electric and Hybrid Vehicles," Power Electronics, IEEE Transactions on, vol. 28, pp. 2151-2169, 2013.

[18] L. Chuang, G. Bin, L. Jih-Sheng, W. Mingyan, J. Yanchao, C. Guowei, et al., "High-Efficiency Hybrid Full-Bridge&-Half-Bridge Converter With Shared ZVS Lagging Leg and Dual Outputs in Series," Power Electronics, IEEE Transactions on, vol. 28, pp. 849-861, 2013.here is reference. And here is reference. And here is reference. And here is reference. And here is reference.